On the Ground Effect of Static Circular Peripheral Jet

AUTHOR(S):

MAEDA, Hiroshi; KAWANO, Yousuke

CITATION:

MAEDA, Hiroshi ...[et al]. On the Ground Effect of Static Circular Peripheral Jet. Memoirs of the Faculty of Engineering, Kyoto University 1967, 29(1): 46-57

ISSUE DATE:

1967-03-31

URL:

http://hdl.handle.net/2433/280680

On the Ground Effect of Static Circular Peripheral Jet

By

Hiroshi MAEDA* and Yousuke KAWANO*

(Received September 30, 1966)

As a part of general investigations into Ground Effect Machine (GEM), a study has been made related to the jet flow and the base pressure of a circular peripheral jet in proximity to the ground. Approximate theories have been derived by using simple assumptions to obtain the relations between the jet flow or the base pressure and the hover height above the ground.

The theoretical results are compared with the experiment of a circular peripheral jet model GEM. The agreement between those results are not so excellent, but it is supposed that the reason depends mainly on the viscous effects which are neglected in this analysis.

1. Introduction

It is well-known that the base pressure surrounded in proximity to the ground with a peripheral jet is increased considerably, and those phenomena have recently been utilized to ground effect machines. However the theoretical and experimental investigations have been carried out mainly for two-dimensional GEMs, and therefore, from the practical stand point a study for three-dimensional GEMs with circular peripheral jet (i.e. axi-symmetric peripheral jet) has been tried here. In this paper, two theoretical treatments have been developed for a circular peripheral jet, i.e. the simple momentum theory and the thin jet thoery, as though they had been extended for the analysis of GEMs with two-dimensional jet[1].

For the simplification of calculation, the assumptions are given as follows:

1) The jet flow is steady, invisid-incompressible and axi-symmetrical.
2) The base pressure P_b is uniform within the cavity.
3) The velocity distribution of the jet is uniform at the exit from the slot.
4) The supply pressure H_e is constant across the exit.
5) Jet momentum J is constant.

2. Theoretical Analysis

2.1 Dimensional Analysis of the Flow

Let us consider the flow shown in Fig. 1, in which a circular peripheral jet

* Department of Aeronautical Engineering.

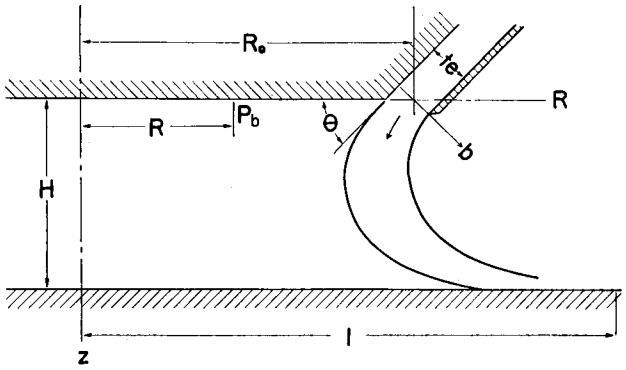

Fig. 1. Theoretical flow model of circular peripheral jet.

emitted from the slot with inclined angle reattaches to the ground. If the ratio of the supply pressure to the ambient pressure is not so large, the flow may be treated as incompressible. The base pressure of the GEM's bottom at distance R from the center is expressed as the following non-dimensional form

$$C_{pb} \equiv (P_b - P_\infty)/(H_e - P_\infty)$$

C_{pb} is considered to be a function of six non-dimensional combinations of the parameters and hence may be written[2)]

$$C_{pb} = f\{\theta,\ H/t_e,\ R/t_e,\ R_0/t_e,\ l/t_e,\ [(H_e - P_\infty)\, t_e^2/\rho\nu^2]^{1/2}\} \qquad (1)$$

In some practical cases it is possible to simplify this equation, i.e. if the length of the ground l is sufficiently large compared with R, l has no effect on the base pressure. In other words, the parameter l/t_e is no longer important and may be discarded from the equation (1). Furthemore, if Reynolds number $R_e = [(H_e - P_\infty) t_e^2/\rho\nu^2]^{1/2}$ is sufficiently large, the flow may be expected to become insensitive to variations of fluid viscosity, so that Reynolds number may be omitted from the equation.

After these simplifications, the equation (1) becomes

$$C_{pb} = f\{\theta,\ H/t_e,\ R/t_e,\ R_0/t_e\} \qquad (2)$$

2.2 Simple Momentum Theory

A theoretical flow model of the circular peripheral jet is shown in Fig. 1. From the assumption given previously and the Bernoulli theorem, the following relation is held on the jet flow. i.e. $\rho u^2 = 2(H_e - P_\infty) = \text{Const}$,

Furthemore, two other important relations, obtained by the equilibrium condition between the jet momentum and the pressure forces are as follows:

$$L = (P_b - P_\infty) S' + J \sin\theta \tag{3}$$

$$2\pi(R_0 - \tfrac{1}{2} t_e \operatorname{cosec}\theta) H(P_b - P_\infty) = J(1+\cos\theta) \tag{4}$$

From the equations (3) and (4), the non-dimensional augmentation parameters of the base pressure and the lift are calculated as follows:

$$C_{pb} = (P_b - P_\infty)/(H_e - P_\infty) = \frac{2R_0/t_e(1+\cos\theta)}{(R_0/t_e - \frac{1}{2}\operatorname{cosec}\theta) H/t_e} \tag{5}$$

$$C_L = L/\pi R_0^2 (H_e - P_\infty) = (1 - \tfrac{1}{2} t_e/R_0 \operatorname{cosec}\theta)^2 C_{pb} + 4 t_e/R_0 \sin\theta \tag{6}$$

It should be noted that the equation (5) indicates that the augmentation of the base pressure increases without limits as the hover height above the ground decreases. Thus, in this theory both the augmentations of the base pressure and the lift would approach infinity as the hover height is reduced to zero.

2.3 Thin Jet Theory

Let us consider a jet flow model as shown in Fig. 2. The simplified force balance equation between centrifugal and pressure forces expressed across a jet element is as follows:

$$\rho R d\phi ds\, tu^2/r = R d\phi\, ds (P_b - P_\infty)$$

or

$$1/r = (P_b - P_\infty)/\rho u^2 t \tag{7}$$

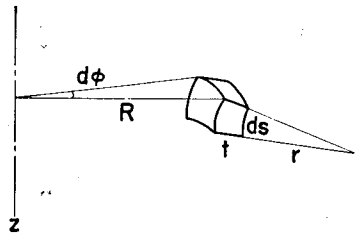

Fig. 2. Jet element.

Using the assumption above-stated, the simplified force balance equation (7) is reduced to

$$r \cdot R = 2/C_{pb} \cdot R_0 t_e \tag{8}$$

where, r is a radius of curvature of the jet flow and it is expressed by

$$r = \frac{[1 + (dz/dR)^2]^{3/2}}{d^2 z/dR^2}$$

Furthemore, using a non-dimensionalized co-ordinate, such that

$$x = R/t_e \quad \text{and} \quad y = z/t_e$$

the simplified force balance equation (7) is finally reduced to

$$y''/(1+y'^2)^{3/2} = 2Cx \tag{9}$$

where, y' and y'' denote dy/dx and d^2y/d^2x respectively and C is given by

$$C = C_{pb}/4 \cdot t_e/R_0$$

Integraing the equation (9)

$$y'/(1+y'^2)^{1/2} = Cx^2+a \tag{10}$$

The integration constant a is determined from the boundary condition at the jet exit, i.e.

$$y' = -\tan\theta \quad \text{at} \quad x=R_0/t_e-\tfrac{1}{2}\operatorname{cosec}\theta$$

Thus

$$a = -[\tan\theta/(1+\tan^2\theta)^{1/2}+C(R_0/t_e-\tfrac{1}{2}\operatorname{cosec}\theta)^2]$$

The equation (10) is therefore rearranged as follows:

$$y'^2 = \frac{(x^2-r^2)^2}{(\alpha^2-x^2)(x^2-\beta^2)} \tag{11}$$

where,

$$\alpha^2 = 4R_0/C_{pb}t_e[\tan\theta/(1+\tan^2\theta)^{1/2}+C_{pb}t_e/4R_0(R_0/t_e-\tfrac{1}{2}\operatorname{cosec}\theta)^2+1]$$
$$\beta^2 = 4R_0/C_{pb}t_e[\tan\theta/(1+\tan^2\theta)^{1/2}+C_{pb}t_e/4R_0(R_0/t_e-\tfrac{1}{2}\operatorname{cosec}\theta)^2-1]$$
$$r^2 = 4R_0/C_{pb}t_e[\tan\theta/(1+\tan^2\theta)^{1/2}+C_{pb}t_e/4R_0(R_0/t_e-\tfrac{1}{2}\operatorname{cosec}\theta)^2]$$

From the equation (11), the denominator must be non-negative because y' should be real, i.e.

$$(\alpha^2-x^2)(x^2-\beta^2)\geqq 0 \tag{12}$$

If the unbounded region $x>0$ is considered, from the equation (12), the following condition must be held, i.e.

$$\beta \leqq x \leqq \alpha$$

Under these considerations, the equation (11) is reduced as follows:

$$y' = \pm\left[\frac{x^2-r^2}{\sqrt{(\alpha^2-x^2)(x^2-\beta^2)}}\right] \tag{13}$$

Integrating the equation (13), the integral domain is separated as shown in Fig. 3. It is clear that at $\beta\leqq x\leqq r$

$$y' = +\left[\frac{x^2-r^2}{\sqrt{(\alpha^2-x^2)(x^2-\beta^2)}}\right]<0$$

at $\quad 0\leqq y\leqq y_0 \qquad (14)$

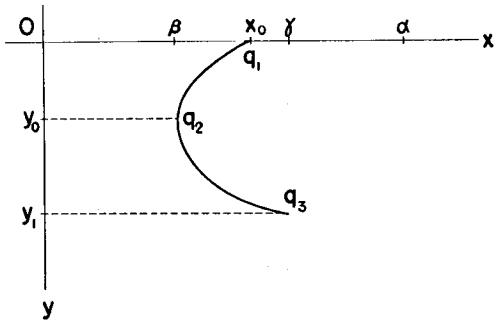

Fig. 3. Stream line.

$$y' = -\left[\frac{x^2-r^2}{\sqrt{(\alpha^2-x^2)(x^2-\beta^2)}}\right] > 0 \quad \text{at} \quad y_0 \leqq y \leqq y_1 \tag{15}$$

i) The domain from q_1 to q_2

The boundary condition is

$$y = 0 \quad \text{at} \quad x = x_0 = R_0/t_e - \tfrac{1}{2}\operatorname{cosec}\theta$$

The equation (14) can be integrated such that

$$\int_0^y dy = \int_{x_0}^x \frac{x^2-r^2}{\sqrt{(\alpha^2-x^2)(x^2-\beta^2)}}dx \tag{16}$$

The equation (16) can be expressed in terms of elliptic functions, i.e.

$$y = \alpha[E(\varphi_0, k) - E(\varphi, k)] - r^2/\alpha[F(\varphi_0, k) - F(\varphi, k)] \tag{17}$$

where,

$$F(\varphi, k) = \int_0^\varphi \frac{d\varphi}{\sqrt{1-k^2\sin^2\varphi}} \qquad \text{The elliptic integral of the first kind}$$

$$E(\varphi, k) = \int_0^\varphi \sqrt{1-k^2\sin^2\varphi}\,d\varphi \qquad \text{The elliptic integral of the second kind}$$

$$k^2 = \frac{\alpha^2-\beta^2}{\alpha^2}, \quad \varphi = \sin^{-1}\sqrt{\frac{\alpha^2-x^2}{\alpha^2-\beta^2}}, \quad \varphi_0 = \sin^{-1}\sqrt{\frac{\alpha^2-x_0^2}{\alpha^2-\beta^2}}$$

ii) The domain from q_2 to q_3

Also the equation (15) can be integrated

$$\int_{y_0}^y dy = -\int_\beta^x \frac{x^2-r^2}{\sqrt{(\alpha^2-x^2)(x^2-\beta^2)}}dx \tag{18}$$

where y_0 is a constant determined from the equation (17), substituting

$$x = \beta, \qquad \text{i.e.} \quad \varphi = \pi/2$$

Similarly the equation (18) can be expressed such that

$$y - y_0 = -\alpha[E(\varphi_1, k) - E(\varphi, k)] + r^2/\alpha[F(\varphi_1, k) - F(\varphi, k)] \tag{19}$$

Furthermore it is clear that the stream line borders on the ground at $x=r$, i.e.

$$y' = 0 \qquad \text{at} \qquad x = r$$

namely in the equation (19)

$$\varphi_1 = \sin^{-1}\sqrt{\frac{\alpha^2-r^2}{\alpha^2-\beta^2}} = \pi/4$$

Finally

$$y_1 = \alpha[E(\varphi_0, k)+E(\pi/4, k)-2E(\pi/2, k)]+r^2/\alpha[2F(\pi/2, k)-F(\varphi_0, k)-F(\pi/4, k)] \tag{20}$$

Next, let us calculate the lift force L. Refering the relation (3).

$$L = (H_e-P_\infty)S'C_{pb}+J\sin\theta$$

Thus

$$C_L = (1-\tfrac{1}{2}\, t_e/R_0 \operatorname{cosec}\theta)^2 C_{pb}+4t_e/R_0 \sin\theta \tag{21}$$

It must be born in mind that C_{pb} is not represented explicitly in the equation (20). In short, the hover height above the ground is determiend from the equation (20) depending on the base pressure.

3. Results and Discussion

A model and the measuring instrument which were used to investigate the jet flow and base pressure are shown in Fig. 4. The experiment was carried out to

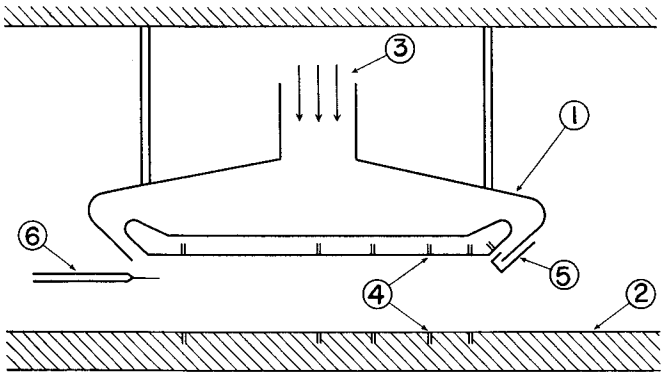

Fig. 4. Model and measuring instrument.

determine the pressure distributions on the bottom surface of GEM and the ground surface respectively. The variable parameters are hover heights above the ground and the jet velocities or accordingly the Reynolds numbers. As has been stated previously, the assumptions of large ground area and high Reynolds numbers are satisfied in this experiment. Furthermore, since the relation of $H_e/P_\infty < 1.05$ is satisfied at any time, the incompressible flow conditions is also held throughout the

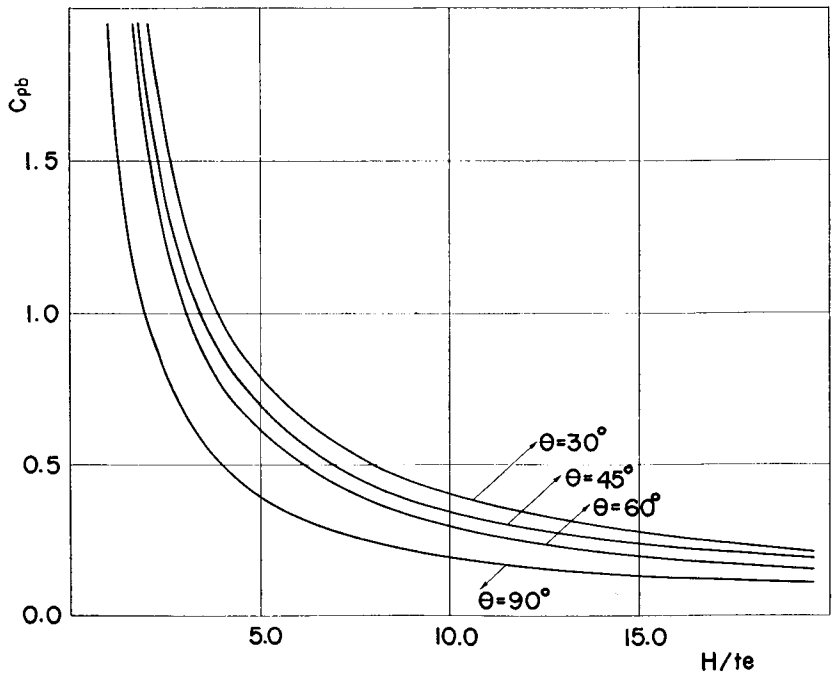

Fig. 5. Pressure coefficient (Simple momentum theory).

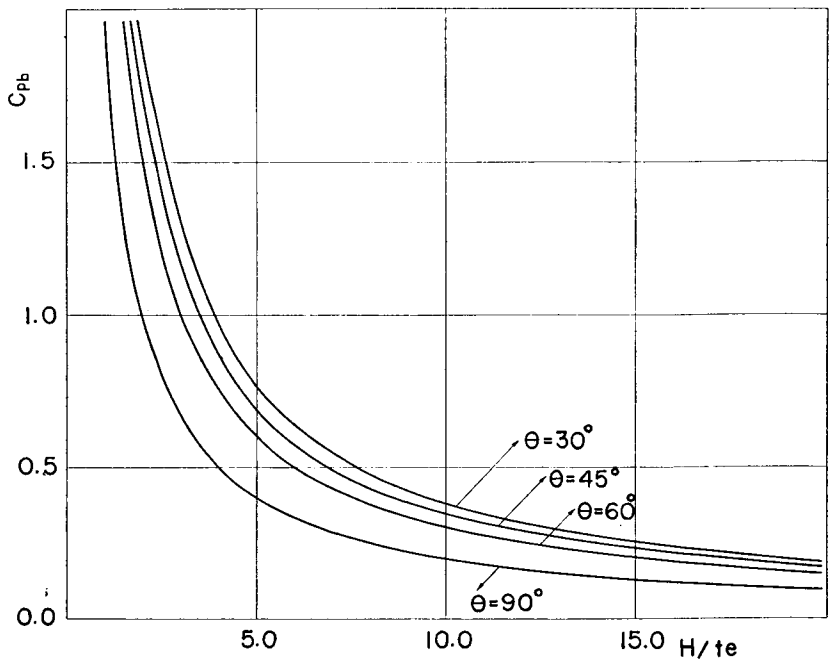

Fig. 6. Pressure coefficient (Thin jet theory).

experiments. The inclined angle of jet slot, θ, jet slot width, t_e, and the radius of GEM's bottom surface, R_0, are all constant and the numerical values of the model are as follows;

$$\theta = 45^\circ, \quad t_e = 5 \text{ mm}, \quad R_0 = 200 \text{ mm}$$

Fig. 5 and Fig. 6 illustrate the variations of C_{pb} corresponduing to H/t_e calculated by the simple momentum theory and the thin jet theory respectively. The relations are given by the equations (5) and (20) respectively, and the parameter of various curves is the inclined angle θ. Comparing Fig. 5 with Fig. 6, it is noticed that the agreement between the results of the simple momentum theory and the thin jet theory is well. Therefore, the lift coefficient, C_L, is only calculated with the simple momentum theory, or by the equation (6), and the relation between C_L and H/t_e is shown in Fig. 7. In this diagram, the curves correspond to the various angles, too.

The base pressure distribution measured on the GEM's bottom surface are plotted in Fig. 8, for various values of H/t_e and Reynolds numbers. It is clear that the pressure distribution is not uniform when the values of H/t_e and R/t_e become large. The pressure distribution on the surface of the ground board is also measured and shown in Fig. 9.

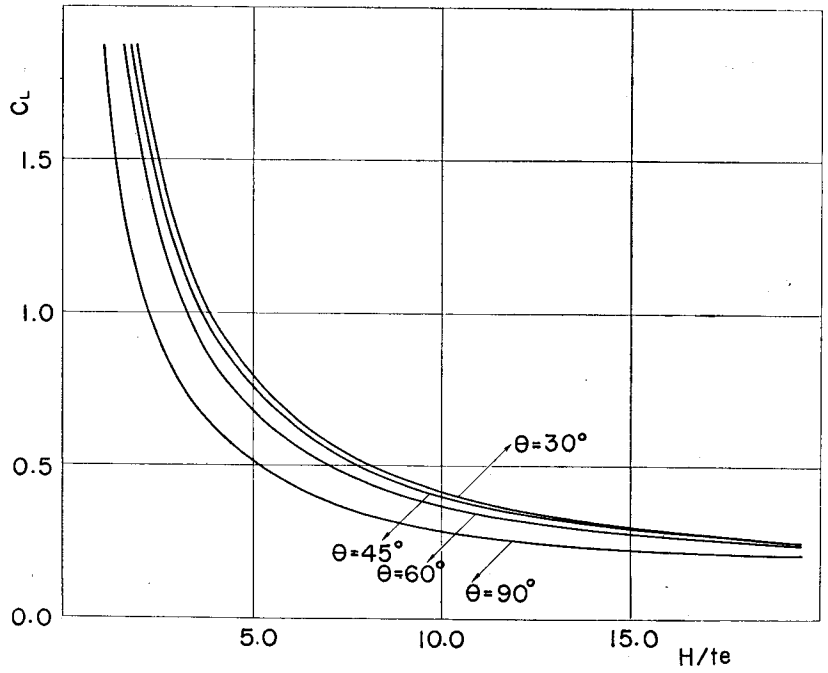

Fig. 7. Lift coeffidient (Simple momentum theory).

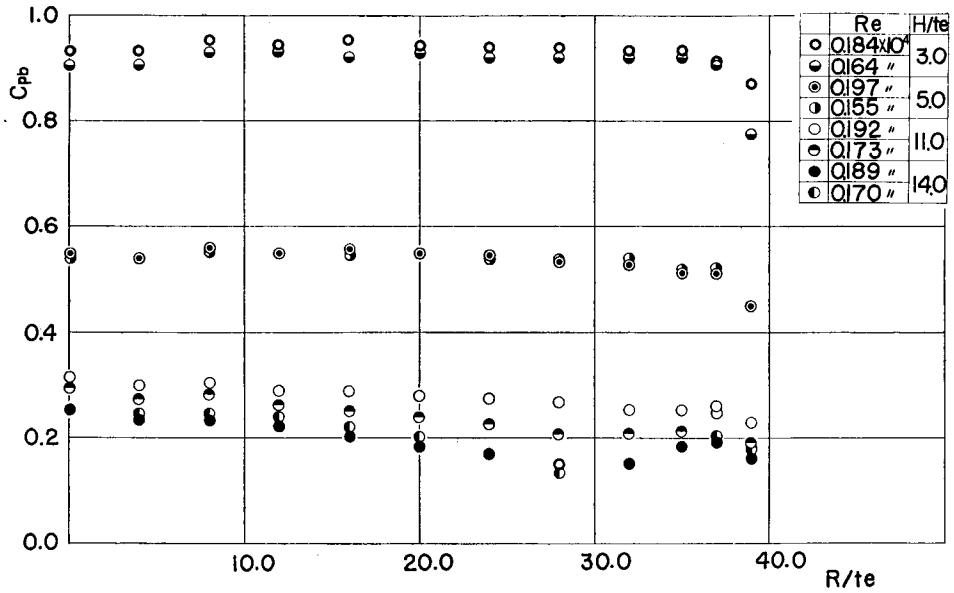

Fig. 8. Pressure distribution on GEM's bottom.

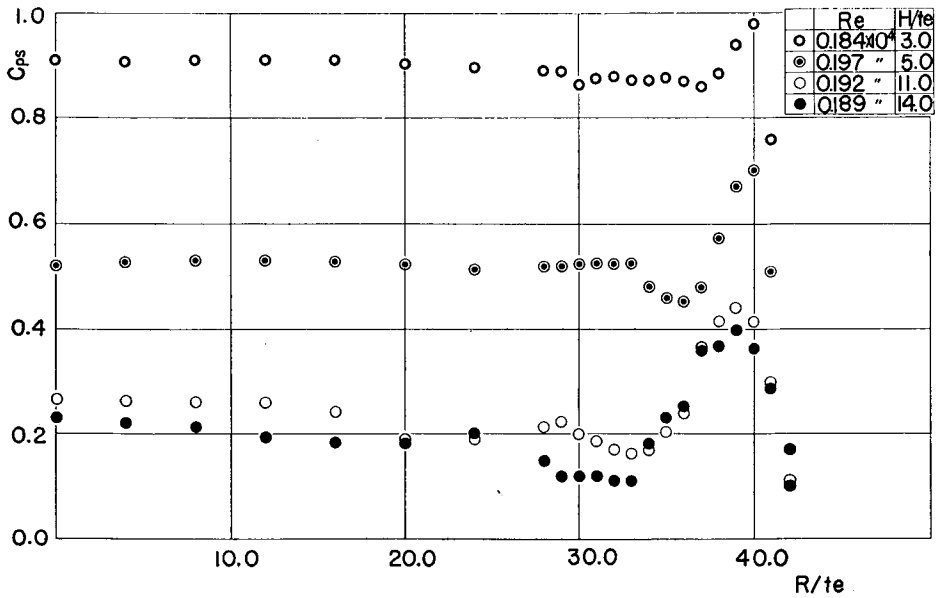

Fig. 9. Pressure distribution on ground surface.

Comparing the latter result with the values of the base pressure on the GEM's bottom surface, the agreement between those values is good except the region close to the peripheral jet flow. Those experimental results indicate that the pressure distributions in the high pressure chamber surrounded by the GEM's bottom and ground surface are roughly constant and the assumption of constant base pressure seems to be valid. However, in the case of circular or three-dimensional GEM, the area close to the peripheral jet is much larger than that of the two-dimensional jet, and therefore the nonuniformity above stated will affect C_{pb} or C_L considerably.

The average pressure coefficients C_{pb} are calculated with the experimental results stated above and are plotted in Fig. 10. In this diagram the analytical

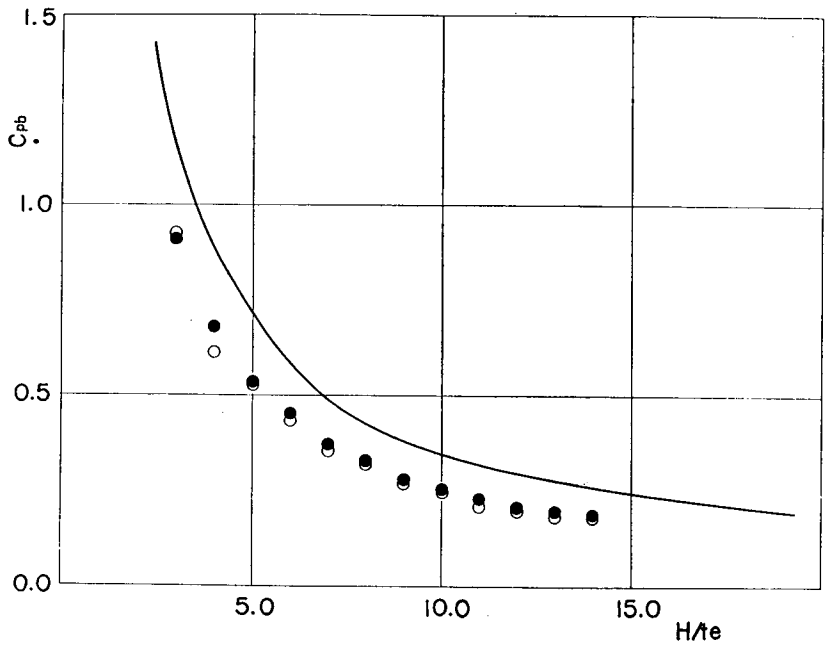

Fig. 10. Average pressure coefficient.

curve is derived by the use of the thin jet theory or the equation (20). The disagreement between the experimental and analytical results is mainly due to the viscous effect and the thin jet assumptions as well as the two-dimensional cases.

In Fig. 11, the velocity profile at the jet exit is shown nondimensionally, which was used to calculate jet momentum.

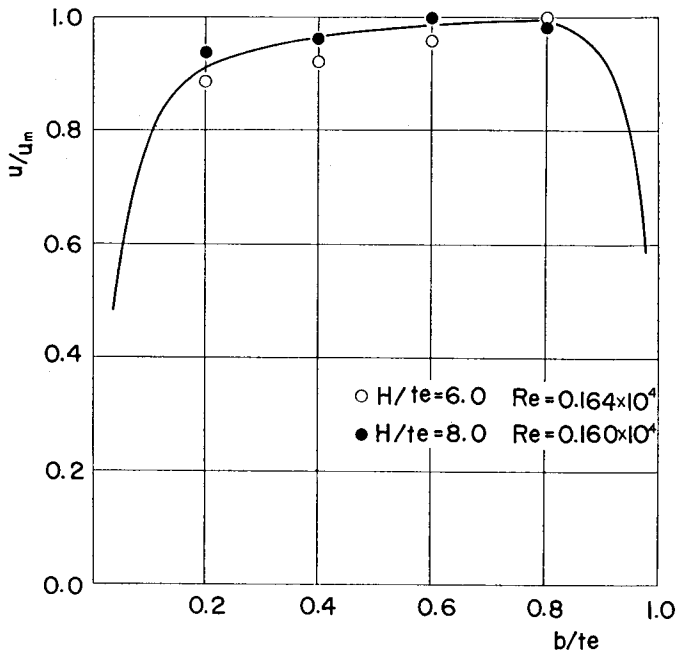

Fig. 11. Velocity profile at exit.

4. Conclusions

The base pressure enveloped with incompressible circular peripheral jet is associated with hover height above the ground.

The dimensional analysis indicates that the base pressure becomes independent of high Reynolds numbers for various values of H/t_e. The uniformity of the base pressure breaks down considerably near the jet, i.e. the base pressure near the jet is found to have a considerable effect on the entrainment properties of the jet due to viscosity.

In two theories given previously, the theoretical results agree comparatively with the experimental results for high values of H/t_e. However there is a great imperfection in the two theores, that is, the theoretical base pressure P_b exceeds the supply pressure H_e. This imperfection may be caused by neglecting jet thickness, i.e. the static pressure in the jet is assumed to be a constant equaled to the ambient pressure. Therefore it is necessary to treat the jet thickness in the future.

Notation

R_0 : radius of model
θ : slot inclined angle
l : length of ground

t_e : width of slot
H : hover height above the ground
S' : base area of GEM's bottom surface
H_e : supply pressure
P_∞ : ambient pressure
P_s : static pressure on the surface of GEM's bottom
P_g : static pressure on the surface of ground
$u_{\max}$: maximum velocity at exit
u : jet velocity
J : jet momemtum, $J=2\pi R\rho tu^2$
ρ : density of the fluid
ν : kinematic viscosity of the fluid
C_{pb} : base pressure coefficient
C_L : lift coefficient
R_e : Reynolds number

References

1) T. Strand; Inviscid-incompressible-Flow of Static Peripheral Jets in Proximity to the Ground, Jour. Aero. Sci. Vol. 28 No. 1 Jan. (1961).
2) C. Bourque and B.G. Newmann; Reattachment of a Two-Dimensional, Incompressible Jet to an Adjacent Flat Plate, The Aero. Quart. Vol. 11 Aug. (1960).